Molecular dynamics simulations of the ribosome

Karissa Y. Sanbonmatsu, Scott C. Blanchard and Paul C. Whitford

To manufacture proteins encoded in the mRNA, the ribosome must convert the sequence of nucleotides inscribed on the mRNA to the sequence of amino acids that comprise the corresponding protein (Fig. 1). That is, the ribosome must translate the four-letter language of nucleic acids into the twenty-letter language of proteins. The ribosome uses a suite of translating molecules (tRNAs) as a molecular look-up table, allowing it to convert from mRNA to protein. Each tRNA carries an amino acid corresponding to a three-nucleotide codon, which may appear in the sequence on the mRNA. In addition, each tRNA has a three-nucleotide anticodon, cognate (through Watson-Crick base pairing) to the corresponding codon in the mRNA. At any given time during elongation, the ribosome exposes one codon in the message to solution. The ribosome must then select only tRNAs with amino acids that correspond to that codon, while rejecting all other tRNAs. Subsequently, the ribosome must move itself along the message by exactly three nucleotides to prepare for the next tRNA. The feat of discriminating between correct and incorrect amino acids, and moving large ligands (~60 Å in length from anticodon to elbow) through the ribosome, from site to site with exquisite precision, has perplexed researchers for almost half a century. Recent studies have been able to quantify the stochastic nature of these processes [1-4] and conclude that the ribosome is highly dynamic in nature.

For elongation to occur, tRNAs must bind to the ribosome, move into the A site, proceed to the P site, continue to the E site, and dissociate from the ribosome. [5] The inner structure of the ribosome produces precise alignment of the tRNA with the mRNA codon of the 30S (Fig. 2) and the peptidyl transferase center on the 50S (Fig. 3). [6-9] On the 50S in particular, the 3'-CCA end of the tRNA is surrounded by a dense thicket of ribosomal RNA in the A site and the P site (Fig. 4). In the E site, nucleotides of the 3'-CCA end are intercalated between two ribosomal nucleotides.[10; 11] The precise alignment of tRNA in each state presents a paradox: how can the tRNA be surrounded by many specific ribosome interactions, yet move to two other completely different states with equally complex interactions? The solution to this paradox is that both the ribosome and the tRNA are extremely dynamic, as evidenced by single-molecule FRET (smFRET), cryo electron microscopy (cryo-EM) and X-ray crystallography data. [2-4; 12-15] While smFRET provides excellent information on the dynamics of the ribosome, it has low spatial resolution. Cryo-EM and crystallographic studies provide higher resolution spatial information but provide little information about dynamics. Molecular dynamics simulations help to bridge the gap between single molecule dynamics experiments and structural biology studies.

With regard to medical applications, the bacterial ribosome is a major target of antibiotics. Approximately 50% of antibiotics used in US hospitals target the ribosome. [16] Although the molecular mechanism of several new antibiotic targets remains obscure, the major classes affect elongation events including decoding,

peptide bond formation and/or translocation. [17-20] A major problem for national health is multi-drug resistant bacteria. Mechanistic studies of the ribosome will help to find new combination therapies that can be used to combat resistant bacteria. Specifically, molecular dynamics simulations shed new light on the conformational transitions between states that occur during protein synthesis. A future class of antibiotics could be those that target transitions, rather than the major states of the ribosome.

tRNA dynamics

The tRNA itself shows large fluctuations during translation. It binds to the ribosome in a highly kinked configuration called the A/T state where the 'A' represents the anticodon interacting with the 30S subunit A site and the 'T' represents the ternary complex interacting with the 50S subunit at the GTPase activity center (Figure 5).[21; 22] Single molecule FRET studies also show rapid tRNA fluctuations between several intermediates occurring before accommodation, where the tRNA moves into the fully bound 'A/A' position (anticodon interacting with the 30S A site and 3'-CCA end interacting with the 50S A site). These include transitions between the initial binding configuration, the codon-anticodon recognition configuration, the GTPase activation configuration and the A/T state. This led to the conclusion that the aminoacyl-tRNA samples a broad ensemble of configurations prior to accommodation.[23]

In addition to tRNA selection, cryo-EM reconstructions of intermediates during translocation demonstrate tRNA flexibility. After accommodation and peptidyl transferase, the tRNA in the A/A position moves to the A/P position (anticodon in 30S A site and 3'-CCA end in 50S P site), while the tRNA in the P/P position moves to the P/E position (anticodon in the 30S P site and 3'-CCA end in the 50S E site). Cryo-EM reconstructions show the tRNA to be in a curved configuration, albeit a curved configuration which differs from the curved configuration required for the A/T position. [24] These two curved configurations are suggestive of an energy storage-release mechanism that allows the tRNA to propel itself through the ribosome. [25] This enthalpic energy source would of course be combined with the source of gated thermal fluctuations resulting from the thermal bath. [26]

The motions of tRNA within the ribosome have been the subject of intense investigation using both bulk and single-molecule techniques. smFRET studies measuring time-dependent changes in the intermolecular distance between A- and P-site tRNAs have proven particularly revealing.[2] During tRNA selection aa-tRNA was shown to enter the A site through reversible excursions between multiple intermediate states. By analyzing the nature of these dynamics for both correct (cognate) and incorrect substates (near-cognate), these dynamics were shown to directly related to the fidelity mechanism. After peptide-bond formation, but prior to translocation, A- and P-site tRNAs within the pre-translocation ribosome complex were shown to undergo reversible exchange processes between kinetically and structurally distinct states. Using structural modeling and traditional mutagenic means, these configurations were shown to correspond to 'Classical' positions, in

which the 3'-CCA ends of A- and P-site tRNAs base pair with the A and P loop rRNA elements at the PTC. In addition, two distinguishable hybrid configurations arising from motions of each tRNA end were observed. Both hybrid configurations result from the motion of the deacylated P-site tRNA towards the E site, where it adopts a P/E configuration [2]. Hybrid tRNA configurations, first demonstrated by Noller and co-workers using chemical footprinting methods ,[5] are key intermediates in the translocation process, lowering the activation barrier for translocation. Analytic treatment of the smFRET data revealed that A- and P-site tRNA motions can occur through independent or coupled processes. The rates of motions observed suggest that A- and P-site tRNA motions entailed large-scale conformational events in the ribosome.

Overall dynamics of the ribosome

In addition to the tRNA, the ribosome itself has been shown to have several dynamic regions. We refer to motion of a region of a subunit with respect to the same subunit as intrasubunit motion. We refer to the motion of the two subunits with respect to each other as intersubunit motion.[27] The most obvious motion performed by the ribosome is the so-called 'ratchet-like' pivoting of the 30S subunit with respect to the 50S subunit (Figure 6). [27] Cryo-EM reconstructions of the 70S ribosome in the presence of EF-G showed a substantial rotation of the 30S relative to its initiator configuration upon EF-G binding. [27] It was previously thought that this motion causes translocation of the tRNA and mRNA through the ribosome. Recent FRET experiments have shown that ratchet-like fluctuations occur at equilibrium in absence of EF-G. [28] EF-G acts to trap the ribosome in the ratcheted position.

Several intrasubunit motions have been observed within the small subunit. The decoding center of the small subunit contains two universally conserved nucleotides: A1492 and A1493. These have been shown to be dynamic in NMR studies[29], fluorescence studies[30] and are observed to be disordered in x-ray crystallography systems. [8; 31]

The head domain of the small subunit has been shown to exist in multiple conformations [14; 32] and also to be dynamic (Figure 7).[14; 28; 33] Cate and co-workers first observed in alternative crystal forms that the head of the small subunit was rotated around a neck region with respect to its body. Spahn and co-workers have shown that this rotation is critical for translocation. [32] In particular, cryo-EM reconstructions of EF-G bound ribosomes have recently shown that two EF-G bound populations exist: one with the 30S body pivoted with respect to the 50S (ratcheted) and a second with the 30S body pivoted and the 30S head rotated (head swiveled). The study shows that while ratchet motion is necessary for translocation, the majority of codon-anticodon translocation movement occurs during 30S head swivel, an approximately orthogonal motion to the 'ratchet-like' pivot of the 30S with respect to the 50S. FRET experiments containing donor-acceptor FRET pairs on small subunit proteins located on the head and body show that the head undergoes significant fluctuations in solution[28; 33].

The mRNA must also be dynamic, although this is difficult to measure. Clearly the mRNA scans the 30S for the correct initiation configuration. The mRNA also moves along the 30S during translocation. It is known that the mRNA is steadied by not only the tRNA anticodons, but also several universally conserved nucleotides on the 30S (*e.g.,* G530, A1492 and A1493). However, it is not known what happens to this configuration during translocation and during initiation.

The 50S has been shown to undergo large intrasubunit conformational changes. The L1 stalk and L7/L12 stalk have been captured in two distinct configurations: factor bound and factor free. [27; 34] Upon ternary complex binding, the L7/L12 stalk moves towards the central protuberance. Upon EF-G binding and ratcheting, the L1 stalk moves towards the central protuberance. Single molecule FRET studies have shown the L1 stalk to undergo enormous and rapid fluctuations that are independent of tRNA fluctuations (Figure 8). [35-37] However, upon EF-G binding, these fluctuations tend to be more synchronized. Because the L1 stalk interacts with the P/E position and E/E position tRNA, it is thought to be involved with E site tRNA dissociation. Single molecule studies also show the L7/L12 stalk to fluctuate rapidly.

The L7/L12 protein complex itself is thought to be the most dynamic region of the ribosome. This consists of a long alpha helix (L10) bolstered by several L7/L12 NTD dimers.[38; 39] Each L7/L12 NTD domain is connected to its CTD by a long disordered flexible linker. These allow the CTD to undergo tremendous large fluctuations which may aid in capturing translation factors in a fly-casting mechanism.[40]

Molecular dynamics simulations and other computational studies of the ribosome

Rapid kinetics, single molecule FRET, x-ray crystallography and cryo-EM have provided an excellent glimpse into the dynamics of the ribosome. To obtain the free energy landscape of the ribosome and a more complete understanding of elongation, this large body of experiments must be integrated into a coherent picture. Molecular dynamics simulation is an excellent tool to provide a theoretical framework to ground interpretation of experimental results.

By labeling strategic regions of the ribosome, rapid kinetics experiments have been able to isolate the various substeps of elongation, giving us the framework for how translation procedes.[41] Single molecule FRET experiments use donor-acceptor label pairs to obtain time-dependent distance constraints on specific conformational changes. [4] X-ray crystallography structures produce high-resolution atomic models of the ribosome in its resting states (classical, EF-G bound, and EF-Tu bound).[7; 10; 14; 42-44] Three-dimensional cryo-EM reconstructions all us to construct atomic models of the ribosome in a wide variety of functional states.[12; 15; 32] Molecular dynamics simulations integrate the above data into a single coherent mechanistic framework. [45]

Modeling efforts[46; 47] and advances in high-performance computing have produced an era in which molecular modeling and simulations can clarify the relationship

between static ribosome structures,[32; 48] structural fluctuations about these local energetic minima,[49; 50] transitions between minima, and ribosome function. [26; 51; 52] Molecular dynamics simulations and modeling studies have explored the decoding center [53-56], isolated tRNA [57] and the inner core of the 30S subunit [58; 59], kink turns[60; 61] , the ribosome tunnel,[62] and drug binding. [63-65] Adaptive-mesh refinement Poisson-Boltzmann studies based on phosphate/C-alpha structures have examined the electrostatic potential of the large and small subunits [66]. Coarse-grained normal mode studies have investigated the motions of the ribosome within the approximations of the Gaussian network model [49; 66; 67]. Real-space refinement has been combined with cryo-EM structures to study the beginning and end states of a conformational change that occurs during translocation [68]. Explicit solvent molecular dynamics simulations have previously helped elucidate functional mechanisms of biomolecular systems [69-73] and have been validated with experiments [74]. Large-scale supercomputers, together with the GROMACS program,[75] have enabled us to simulate the ribosome in explicit solvent (3.2×10^6 atoms) for an aggregate sampling of > 2 microseconds (~2100 ns), producing the largest simulation of a biomolecular complex to date, [45] more than 20-fold larger than previous efforts, which simulated the ribosome for 85 ns [76] and a small portion (1.25×10^5 atoms) for 2.1 microseconds. [77]

The petaFlop barrier was broken several years ago by the Los Alamos RoadRunner machine. Even with such fast supercomputers, a full simulation of the ribosome in explicit solvent for physiological time scales (~ 100 ms – 1 s) is currently not possible. Using current molecular dynamics algorithms, we estimate this would require a $\sim 10^3 - 10^4$ fold speed-up or a 1 – 10 exaFlop machine, which may be available between 2019-2024 according to DOE SCIDAC projections. To examine short time scale stability of hydrogen bonds, we performed standard explicit solvent molecular dynamics simulations of localized regions of the ribosome. [78] To study localized conformational changes we have used exhaustive sampling techniques such as replica exchange explicit solvent molecular dynamics. [64; 79; 80] To study the structural stability and to obtain a baseline for validation of reduced force field techniques, we performed multiple extensive explicit solvent simulations. Finally to study large-scale conformational changes we have used a variety of techniques. As a first step, we used targeted molecular dynamics simulations in explicit solvent to obtain a first look at steric interactions occurring during the large-scale conformational change. These results have been validated experimentally. [81; 82] Next, we used a reduced-potential method, called structure-based simulation. [26; 83-85] These unrestrained simulations allow us to observe spontaneous large-scale conformational changes with an estimated total sampling of ~ 200 ms. To validate, we compare against single molecule FRET, cryo-EM, and X-ray crystallography B-factors.

About a decade ago, we performed a limited explicit solvent study of the fidelity on the ribosome, simulating the tRNA-mRNA-ribosome decoding center complex for ultrafast time scales (~ 10 ns). This study was published several years later. [78] We were able to observe stable cognate (correct) codon-anticodon interactions and

unstable near-cognate (incorrect) codon-anticodon interactions. We concluded that the decoding bases (G530, A1492 and A1493) measure the geometry of the codon-anticodon minihelix minor groove and test the stability of the codon-anticodon interaction. We emphasize that it is impossible to obtain accurate free energies from such short simulations; however this first functional study of the ribosome using molecular dynamics established the foundation for more extensive studies.

We have shown recently that at least 1 microsecond of replica sampling is required for exhaustive sampling of the decoding helix. [64] The 1 microsecond of replica sampling amounts to >> 5 microseconds of standard molecular dynamics.[86] Without exhaustive sampling, the entropic component of the free energy cannot be calculated accurately. In this study, the flipping of nucleotides A1492 and A1493 was studied. Our exhaustive sampling molecular dynamics simulations show that these nucleotides flip into and out of helix 44 of the small subunit when no ligands are bound to the small subunit. Several thousand flips occurred during our simulation. We estimate the barrier in free energy for base flipping of these nucleotides to be on the order of a few kcal/Mol, suggesting that the nucleotides continuously flip until ligands bind, trapping them in the flipped out configuration.[64; 80] We note that the study did not include the large subunit. The 50S may have a stabilizing role on A1492 and A1493.

The decoding center is the target of aminoglycoside antibiotics. [18; 29; 87] These antibiotics bind inside helix 44, preventing A1492 and A1493 from residing in their flipped in conformation. We have shown that rather than an induced-fit scenario, where the drug forces these nucleotides to flip out of their helix, a stochastic gating scenario is more likely. Here, the nucleotides continuously flip in and out. Drug binding traps the nucleotides in their flipped-out state. We note that upon correct tRNA binding, an intricate hydrogen bond network exists between G530, A1492, A1493, the tRNA anticodon, and the mRNA codon. Because G530, A1492 and A1493 sense the Watson-Crick geometry of the codon-anticodon interaction, these nucleotides act as a molecular reading head. Aminoglycosides effectively 'jam' this reading head in the accepting configuration with A1492 and A1493 flipped out of their helix, allowing them to interact productively with the tRNA leading to acceptance of the tRNA into the ribosome ('accommodation'). Thus, the aminoglycoside interaction leads to the incorporation of incorrect amino acids into the nascent protein, producing widespread errors in proteins manufactured by the aminoglycoside-bound ribosome. This fidelity phenotype is known as misreading.

To investigate large-scale conformational changes, we first turned to accommodation, the large-scale conformational change involved in tRNA movement through the ribosome. During this conformational change, the aminoacyl-tRNA moves from the A/T state to the fully bound A/A state. This 70Å movement requires the kinked anticodon arm to relax to its native, linear conformation. As a first step, in 2002-2003, we performed ultrafast explicit solvent targeted molecular dynamics simulations, with a total sampling of ~20 ns. These were published in 2005.[52] The simulations revealed several important features of accommodation that were not

previously identified. Because the 3'-CCA end is single stranded, it is thought to be extremely flexible. Our study showed explicitly that flexibility of the 3'-CCA end is required for accommodation. [52] In particular, the simulation revealed that many steric barriers are present in the accommodation pathway. The 3'-CCA end must be extremely flexible to move from the A/T state into the A/A state. In particular, the 3'-CCA end must navigate the intricate and universally conserved accommodation corridor consisting of large subunit rRNA helices H89, H90 and H92. The accommodation corridor was identified by our simulations.[52] This could not be identified from X-ray crystallography or cryo-EM since these methods do not examine the transition between the A/T and the A/A positions.

In our most recent study, we have simulated spontaneous accommodation events. Here, a structure-based simulation approach was used.[26; 83-85] In particular, a potential defined by the x-ray structure of the ribosome with the aminoacyl-tRNA occupying the A/A state was used. Much like an all-atom Go-model simulation, the tRNA was started in the A/T position. The tRNA and ribosome were then allowed to fluctuate freely under the A/A based potential. Over 1000 accommodation simulations were performed with an estimated total sampling on the order of hundreds of milliseconds. The tRNA was observed to be highly dynamic, undergoing reversible excursions from the A/T state towards the A/A state and back. These same reversible excursions were also observed in single molecule FRET studies of accommodation.[26] We found that H89 must fluctuate to make way for the accommodating tRNA.[26] The study also shows that the 3'-CCA end is so disordered that the 3'-CCA end itself presents an entropic barrier to accommodation.

To further validate our structure-based potential, extensive multiple explicit solvent simulations were performed with total sampling of ~2100 ns. [45] Simulations were performed starting the tRNA in the A/A state and also starting the tRNA in the A/T state. The configurational space sampled in the A/A state explicit solvent simulation was similar to the A/A state basin sampled by the structure-based simulation. Similar results were achieved for the A/T state simulations. We also note that our explicit solvent targeted molecular dynamics simulations sampled regions well within the configurational space defined by the structure-based accommodation study. Average fluctuations of the explicit solvent and structure-based simulations were similar. Both simulations showed agreement with X-ray B-factors, [43] with the exception of the 50S stalks, which have been shown to undergo large amplitude fluctuations by single molecule FRET. [35; 36] These fluctuations cannot be captured by X-ray crystallography.

Finally, we used the structure-based method to investigate L1 stalk fluctuations. We found that enormous fluctuations both in displacement and twist, consistent with the large fluctuations observed by single molecule FRET.

In the case of accommodation, our structure-based simulations display a wide variety of accommodation pathways. The shape of the pathway distribution is determined both by the intrinsic properties of the tRNA and by fluctuations of the ribosome. Furthermore, both the structure-based and explicit solvent simulations

show large ensembles of configurations representing the A/A and A/T positions, consistent with single molecule FRET experiments. Our study reveals that large amplitude reversible excursions of the aminoacyl-tRNA combined with stochastic gating of helix 89 allow for accommodation. For accommodation to occur, the entropic barrier introduced by the 3'-CCA end must be over come by (1) the enthalpic minima of the peptidyl transferase center, which includes a base pair between the 3'-CCA end and a ribosomal nucleotide, (2) the enthalpic minima of the anticodon arm, which releases energy stored during ternary complex binding, and (3) an entropic 'kick' produced by the presence of EF-Tu, which prevents the tRNA from escaping the ribosome. It should be emphasized that while extremely flexible components introduce entropic barriers, they also soften the system relative to a molecular machine consisting of more rigid components. This softening may act to fine-tune the free energy landscape. Overall, simulations have established several principles important for ribosome dynamics: multiple pathways, stochastic gating, large amplitude reversible excursions, and entropic barriers.

We suspect that similar principles operate during translocation. However, in this case, the energy landscape seen by the tRNA is itself dynamic: pivoting of the 30S body with respect to the 50S, swiveling of the 30S head and the opening and closing of various gates will significantly alter the barriers in a dynamic fashion. Recent single molecule FRET experiments suggest that each component of the ribosome fluctuates independently and at different time scales. It is only during the rare moments that these fluctuations occur simultaneously in the proper directions that translocation may occur.[35; 36] Such synchronization is enhanced by the presence of EF-G.

Beginning with energetics, the thermal bath in the environment surrounding the ribosome contains enough energy to move the tRNAs through the ribosome. In the case of factor-free translation, the only chemical reaction occurring is the peptidyl transferase reaction. Thermal fluctuations provide the energy to overcome enthalpic and entropic barriers involved in moving the aminoacyl-tRNA from solution to the accommodated A/A position. Once the peptidyl transferase reaction is complete, the system reaches the point of no return, where thermal fluctuations move the deacylated tRNA through the hybrid state to the exit site. The structure of the ribosome carefully controls this movement allowing the new peptidyl-tRNA to move by exactly one codon. Finally thermal fluctuations allow the deacylated tRNA to exit the ribosome to its entropically favorable state – in solution away from the ribosome. The introduction of factors serves to make this process more efficient.

Figure Captions

Figure 1. Overview of ribosome structure determined by Yusupov and co-workers. Blue, small subunit 16S rRNA. Cyan, small subunit proteins. Magenta, large subunit 23S rRNA. Pink, large subunit proteins. White, large subunit 5S rRNA. Yellow, aminoacyl-tRNA. Red, peptidyl-tRNA.

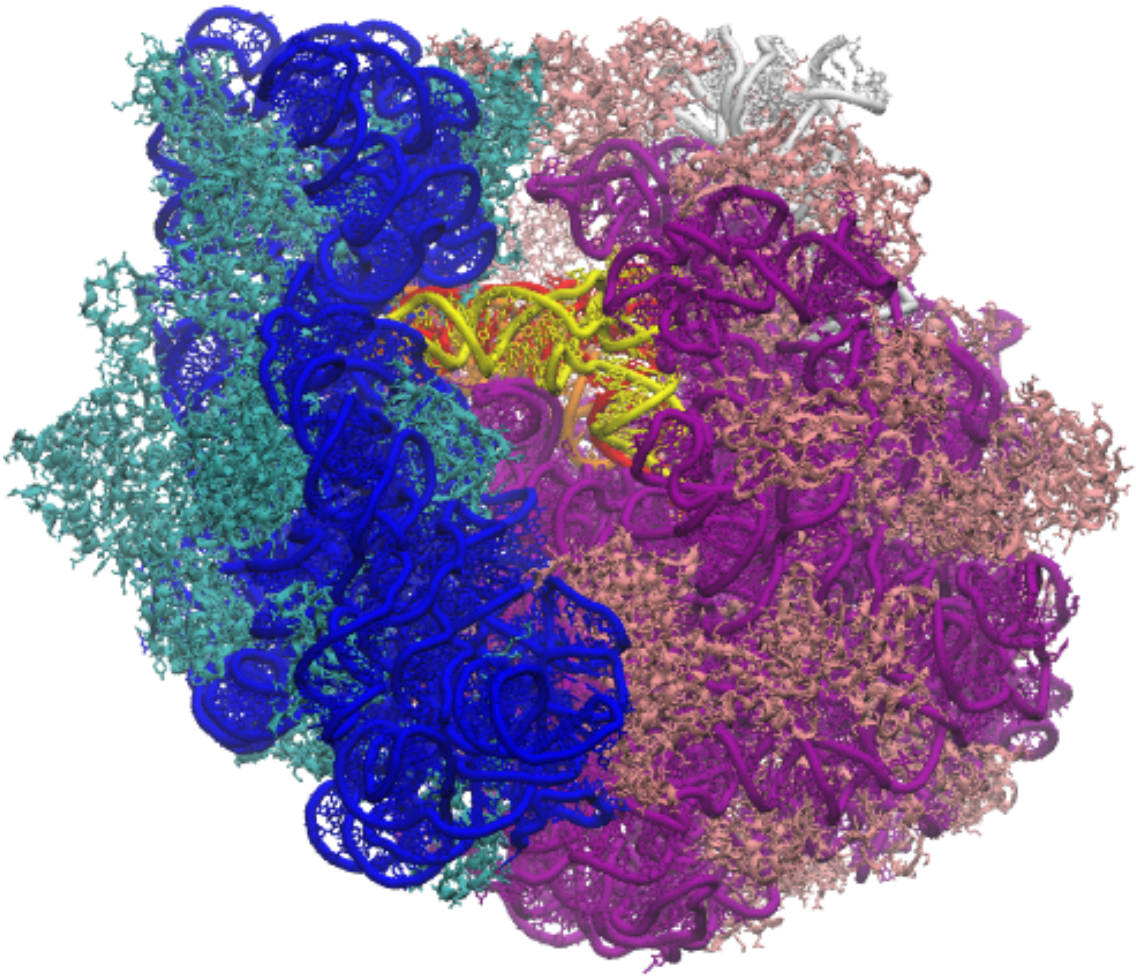

Figure 2. 30S small ribosomal subunit.

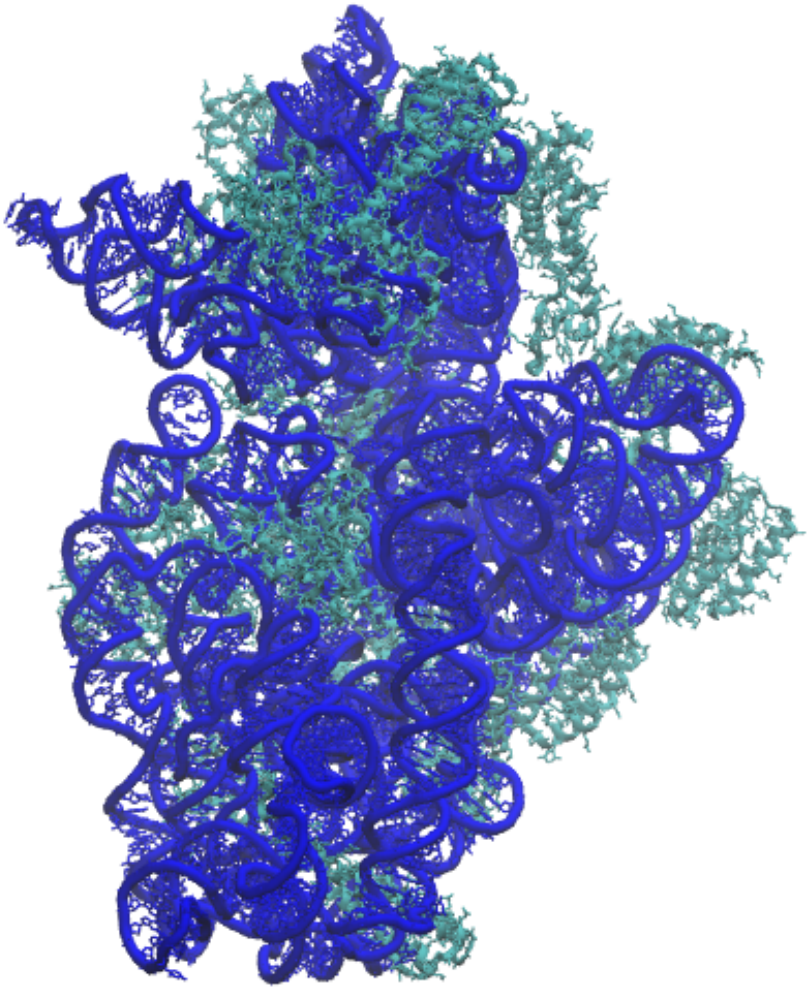

Figure 3. 50S large ribosomal subunit

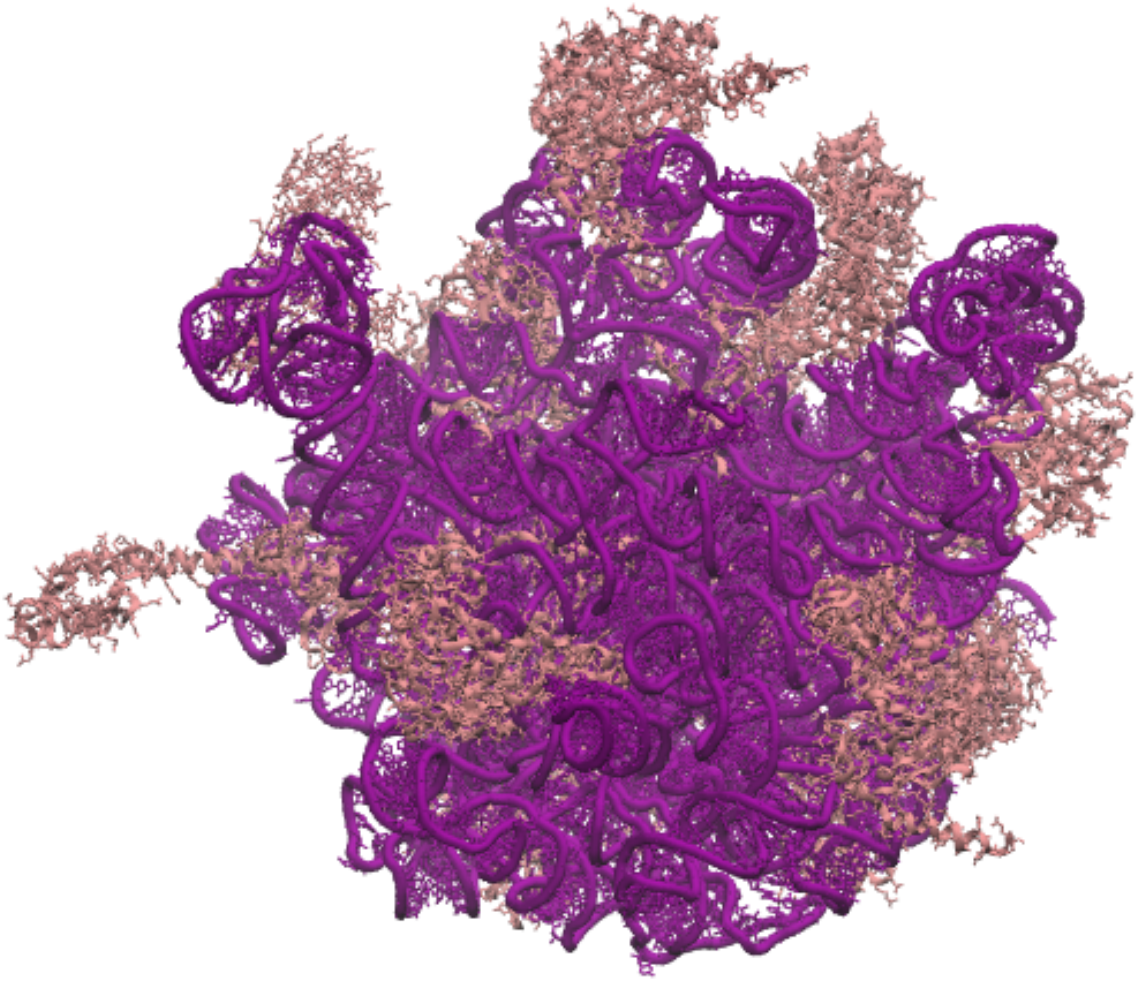

Figure 4. tRNA binding sites on small subunit. Aminoacyl tRNA (yellow) bound to A site. Peptidyl tRNA (red) bound to P site. Exit tRNA (orange) bound to E site.

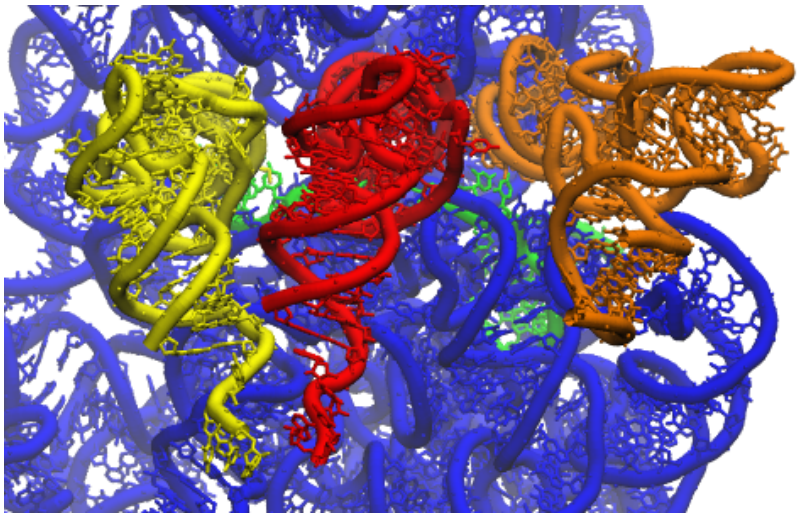

Figure 5. Dynamics of the aminoacyl-tRNA during tRNA selection (accommodation step) in all-atom structure-based simulations. (a) Before accommodation. (b) After accommodation.

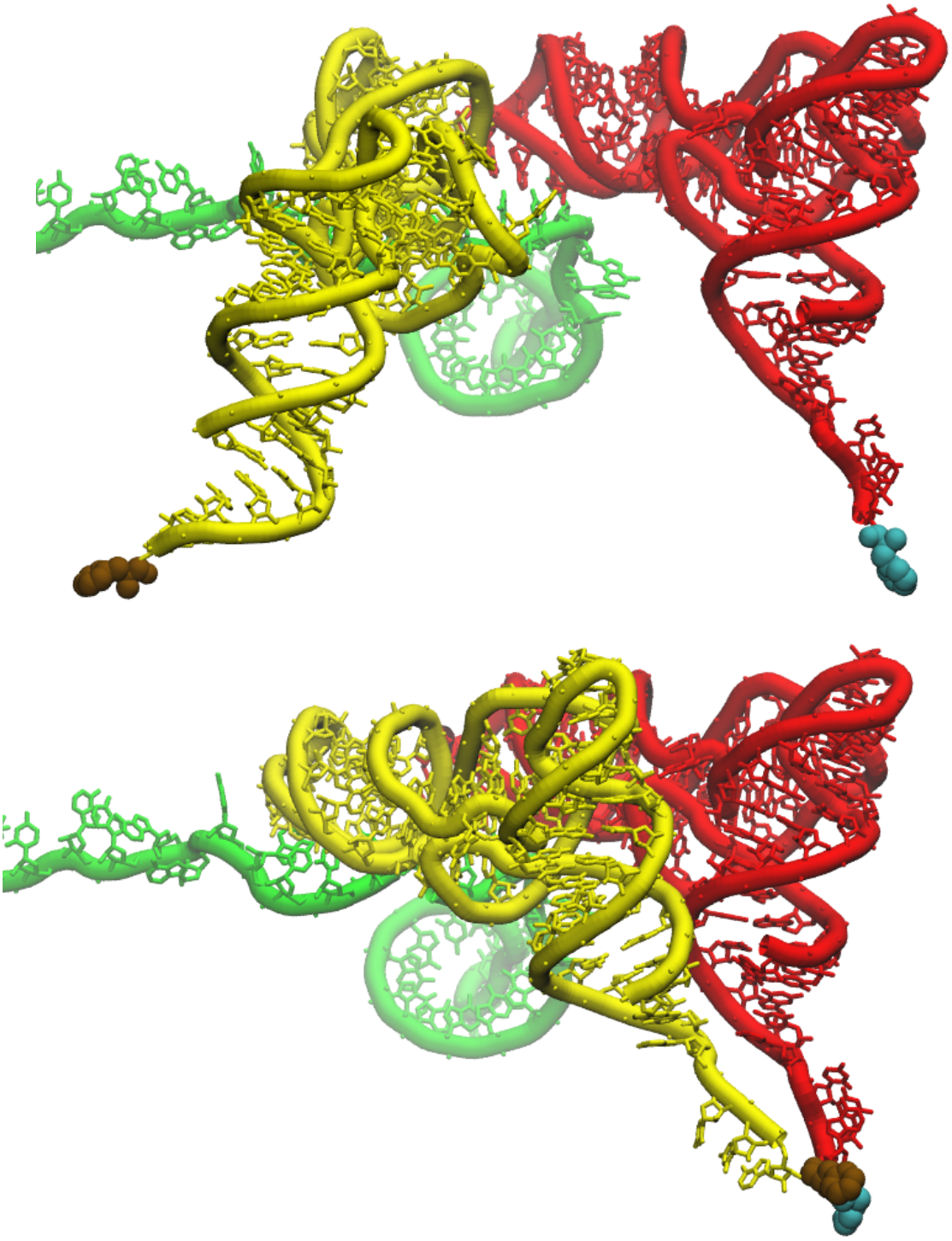

Figure 6. Dynamic regions of the ribosome: pivoting of the 30S with respect to the 50S.

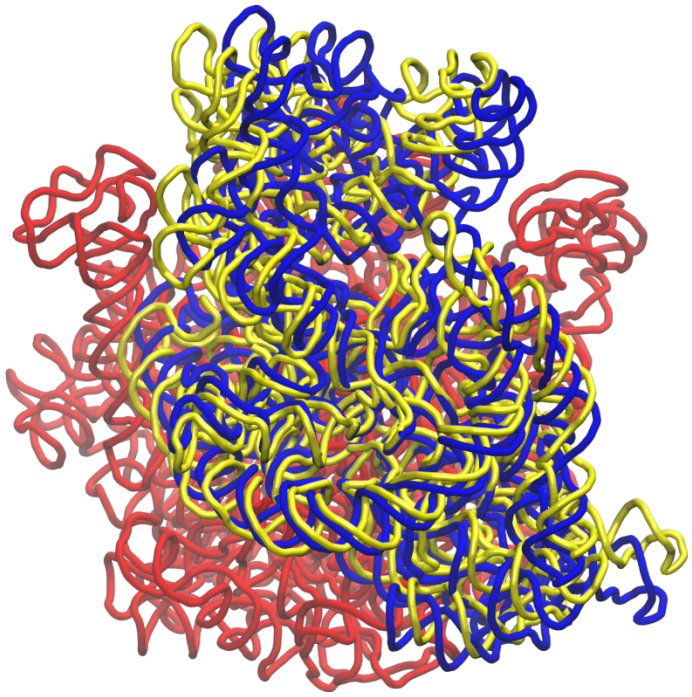

Figure 7. Dynamics of the 30S head swivel in all-atom structure-based simulations.

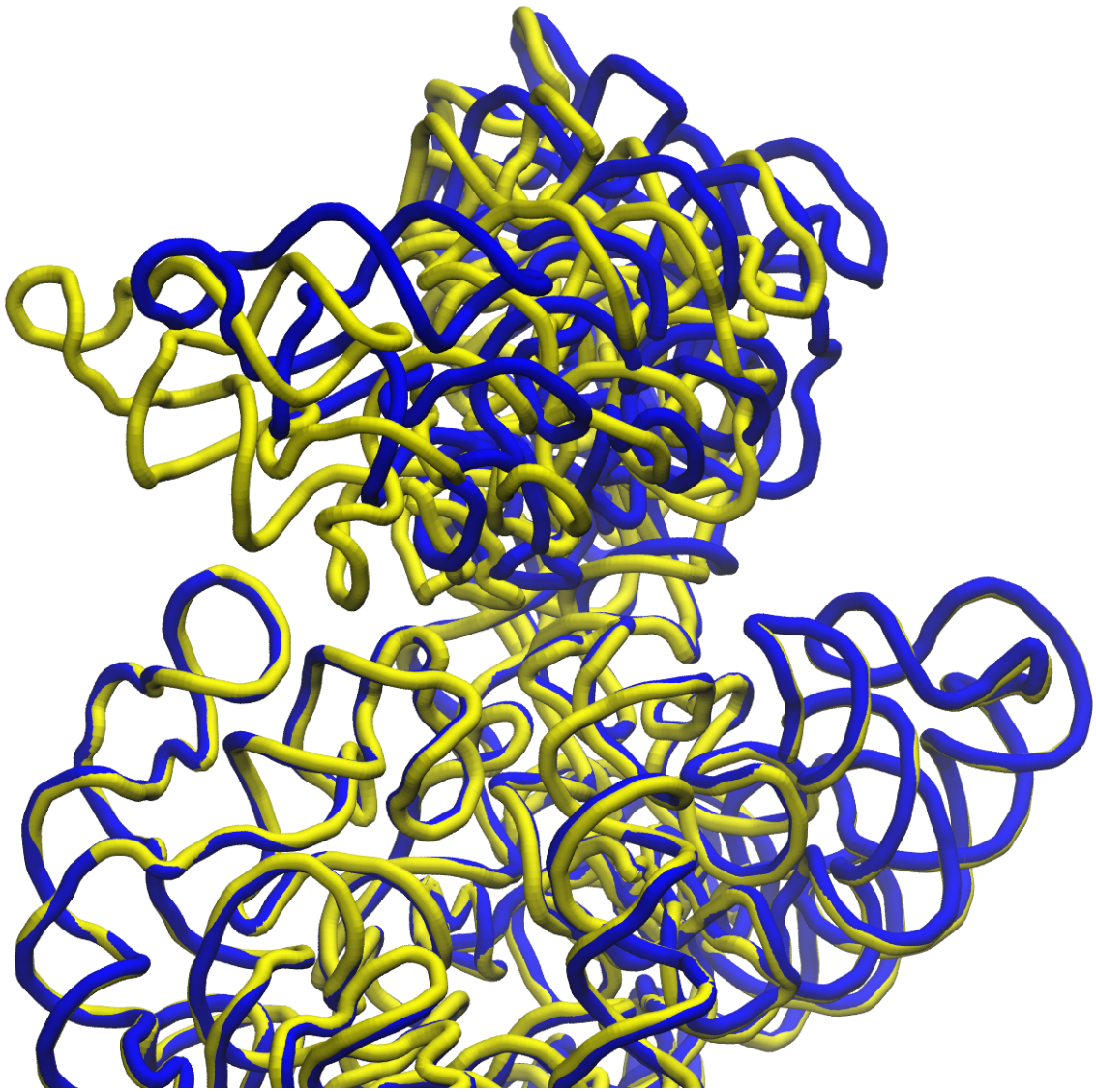

Figure 8. Dynamics of the L1 stalk in all-atom structure-based simulations. Blue and yellow display snapshots of ribosome at different times during simulation.

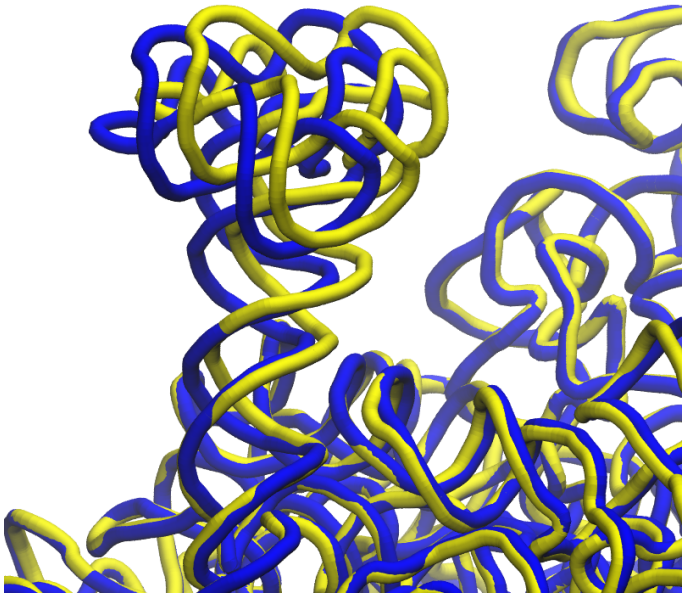

References

1. Feldman, M. B., Terry, D. S., Altman, R. B. & Blanchard, S. C. (2010). Aminoglycoside activity observed on single pre-translocation ribosome complexes. *Nat Chem Biol* **6**, 244.
2. Munro, J. B., Altman, R. B., O'Connor, N. & Blanchard, S. C. (2007). Identification of two distinct hybrid state intermediates on the ribosome. *Mol Cell* **25**, 505-17.
3. Blanchard, S. C., Kim, H. D., Gonzalez, R. L., Jr., Puglisi, J. D. & Chu, S. (2004). tRNA dynamics on the ribosome during translation. *Proc Natl Acad Sci U S A* **101**, 12893-8.
4. Blanchard, S. C. (2009). Single-molecule observations of ribosome function. *Curr Opin Struct Biol* **19**, 103-9.
5. Moazed, D. & Noller, H. F. (1989). Intermediate states in the movement of transfer RNA in the ribosome. *Nature* **342**, 142-8.
6. Demeshkina, N., Jenner, L., Yusupova, G. & Yusupov, M. (2010). Interactions of the ribosome with mRNA and tRNA. *Curr Opin Struct Biol* **20**, 325-32.
7. Yusupova, G., Jenner, L., Rees, B., Moras, D. & Yusupov, M. (2006). Structural basis for messenger RNA movement on the ribosome. *Nature* **444**, 391-4.
8. Ogle, J. M., Brodersen, D. E., Clemons, W. M., Jr., Tarry, M. J., Carter, A. P. & Ramakrishnan, V. (2001). Recognition of cognate transfer RNA by the 30S ribosomal subunit. *Science* **292**, 897-902.
9. Voorhees, R. M., Weixlbaumer, A., Loakes, D., Kelley, A. C. & Ramakrishnan, V. (2009). Insights into substrate stabilization from snapshots of the peptidyl transferase center of the intact 70S ribosome. *Nat Struct Mol Biol* **16**, 528-33.
10. Selmer, M., Dunham, C. M., Murphy, F. V. t., Weixlbaumer, A., Petry, S., Kelley, A. C., Weir, J. R. & Ramakrishnan, V. (2006). Structure of the 70S ribosome complexed with mRNA and tRNA. *Science* **313**, 1935-42.
11. Gao, Y. G., Selmer, M., Dunham, C. M., Weixlbaumer, A., Kelley, A. C. & Ramakrishnan, V. (2009). The structure of the ribosome with elongation factor G trapped in the posttranslocational state. *Science* **326**, 694-9.
12. Zhang, W., Kimmel, M., Spahn, C. M. & Penczek, P. A. (2008). Heterogeneity of large macromolecular complexes revealed by 3D cryo-EM variance analysis. *Structure* **16**, 1770-6.
13. Zhang, W., Dunkle, J. A. & Cate, J. H. (2009). Structures of the ribosome in intermediate states of ratcheting. *Science* **325**, 1014-7.
14. Schuwirth, B. S., Borovinskaya, M. A., Hau, C. W., Zhang, W., Vila-Sanjurjo, A., Holton, J. M. & Cate, J. H. (2005). Structures of the bacterial ribosome at 3.5 A resolution. *Science* **310**, 827-34.

15. Fischer, N., Konevega, A. L., Wintermeyer, W., Rodnina, M. V. & Stark, H. (2010). Ribosome dynamics and tRNA movement by time-resolved electron cryomicroscopy. *Nature* **466**, 329-33.
16. Mankin, A. (2006). Antibiotic blocks mRNA path on the ribosome. *Nat Struct Mol Biol* **13**, 858-60.
17. Blanchard, S. C., Cooperman, B. S. & Wilson, D. N. (2010). Probing translation with small-molecule inhibitors. *Chem Biol* **17**, 633-45.
18. Carter, A. P., Clemons, W. M., Brodersen, D. E., MorganWarren, R. J., Wimberly, B. T. & Ramakrishnan, V. (2000). Functional insights from the structure of the 30S ribosomal subunit and its interactions with antibiotics. *Nature* **407**, 340-348.
19. Schlunzen, F., Zarivach, R., Harms, R., Bashan, A., Tocilj, A., Albrecht, R., Yonath, A. & Franceschi, F. (2001). Structural basis for the interaction of antibiotics with the peptidyl transferase centre in eubacteria. *Nature* **413**, 814-821.
20. Pioletti, M., Schlunzen, F., Harms, J., Zarivach, R., Gluhmann, M., Avila, H., Bashan, A., Bartels, H., Auerbach, T., Jacobi, C., Hartsch, T., Yonath, A. & Franceschi, F. (2001). Crystal structures of complexes of the small ribosomal subunit with tetracycline ; edeine and IF3. *Embo Journal* **20**, 1829-1839.
21. Valle, M., Sengupta, J., Swami, N. K., Grassucci, R. A., Burkhardt, N., Nierhaus, K. H., Agrawal, R. & Frank, J. (2002). Cryo-EM reveals an active role for aminoacyl-tRNA in the accommodation process. *Embo Journal* **21**, 3557-3567.
22. Valle, M., Zavialov, A., Li, W., Stagg, S. M., Sengupta, J., Nielsen, R. C., Nissen, P., Harvey, S. C., Ehrenberg, M. & Frank, J. (2003). Incorporation of aminoacyl-tRNA into the ribosome as seen by cryo-electron microscopy. *Nature Structural Biology* **10**, 899-906.
23. Geggier, P., Dave, R., Feldman, M. B., Terry, D. S., Altman, R. B., Munro, J. B. & Blanchard, S. C. (2010). Conformational sampling of aminoacyl-tRNA during selection on the bacterial ribosome. *J Mol Biol* **399**, 576-95.
24. Connell, S. R., Topf, M., Qin, Y., Wilson, D. N., Mielke, T., Fucini, P., Nierhaus, K. H. & Spahn, C. M. (2008). A new tRNA intermediate revealed on the ribosome during EF4-mediated back-translocation. *Nat Struct Mol Biol* **15**, 910-5.
25. Frank, J., Sengupta, J., Gao, H., Li, W., Valle, M., Zavialov, A. & Ehrenberg, M. (2005). The role of tRNA as a molecular spring in decoding, accommodation, and peptidyl transfer. *FEBS Lett* **579**, 959-62.
26. Whitford, P. C., Geggier, P., Altman, R. B., Blanchard, S. C., Onuchic, J. N. & Sanbonmatsu, K. Y. (2010). Accommodation of aminoacyl-tRNA into the ribosome involves reversible excursions along multiple pathways. *RNA* **16**, 1196-204.
27. Frank, J. & Agrawal, R. K. (2000). A ratchet-like inter-subunit reorganization of the ribosome during translocation. *Nature* **406**, 318-22.
28. Ermolenko, D. N., Majumdar, Z. K., Hickerson, R. P., Spiegel, P. C., Clegg, R. M. & Noller, H. F. (2007). Observation of intersubunit movement of the ribosome in solution using FRET. *J Mol Biol* **370**, 530-40.

29. Fourmy, D., Yoshizawa, S. & Puglisi, J. D. (1998). Paromomycin binding induces a local conformational change in the A-site of 16 S rRNA. *Journal of Molecular Biology* **277**, 333-345.
30. Kaul, M. & Pilch, D. S. (2002). Thermodynamics of aminoglycoside-rRNA Rrecognition: the binding of neomycin-class aminoglycosides of the A site of 16S rRNA. *Biochemistry* **41**, 7695-7706.
31. Berk, V., Zhang, W., Pai, R. D. & Cate, J. H. (2006). Structural basis for mRNA and tRNA positioning on the ribosome. *Proc Natl Acad Sci U S A* **103**, 15830-4.
32. Ratje, R. e. a. (2010). Head swivel on the ribosome facillitates translocation via intra-subunit tRNA hybrid sites. *Submitted*.
33. Majumdar, Z. K., Hickerson, R., Noller, H. F. & Clegg, R. M. (2005). Measurements of internal distance changes of the 30S ribosome using FRET with multiple donor-acceptor pairs: quantitative spectroscopic methods. *J Mol Biol* **351**, 1123-45.
34. Valle, M., Zavialov, A., Li, W., Stagg, S. M., Sengupta, J., Nielsen, R. C., Nissen, P., Harvey, S. C., Ehrenberg, M. & Frank, J. (2003). Incorporation of aminoacyl-tRNA into the ribosome as seen by cryo-electron microscopy. *Nat Struct Biol* **10**, 899-906.
35. Munro, J. B., Altman, R. B., Tung, C. S., Cate, J. H., Sanbonmatsu, K. Y. & Blanchard, S. C. (2010). Spontaneous formation of the unlocked state of the ribosome is a multistep process. *Proc Natl Acad Sci U S A* **107**, 709-14.
36. Munro, J. B., Altman, R. B., Tung, C. S., Sanbonmatsu, K. Y. & Blanchard, S. C. (2010). A fast dynamic mode of the EF-G-bound ribosome. *Embo J* **29**, 770-81.
37. Cornish, P. V., Ermolenko, D. N., Staple, D. W., Hoang, L., Hickerson, R. P., Noller, H. F. & Ha, T. (2009). Following movement of the L1 stalk between three functional states in single ribosomes. *Proc Natl Acad Sci U S A* **106**, 2571-6.
38. Diaconu, M., Kothe, U., Schlunzen, F., Fischer, N., Harms, J. M., Tonevitsky, A. G., Stark, H., Rodnina, M. V. & Wahl, M. C. (2005). Structural basis for the function of the ribosomal L7/12 stalk in factor binding and GTPase activation. *Cell* **121**, 991-1004.
39. Bocharov, E. V., Sobol, A. G., Pavlov, K. V., Korzhnev, D. M., Jaravine, V. A., Gudkov, A. T. & Arseniev, A. S. (2004). From structure and dynamics of protein L7/L12 to molecular switching in ribosome. *J Biol Chem* **279**, 17697-706.
40. Shoemaker, B. A., Portman, J. J. & Wolynes, P. G. (2000). Speeding molecular recognition by using the folding funnel: the fly-casting mechanism. *Proc Natl Acad Sci U S A* **97**, 8868-73.
41. Wintermeyer, W., Peske, F., Beringer, M., Gromadski, K. B., Savelsbergh, A. & Rodnina, M. V. (2004). Mechanisms of elongation on the ribosome: dynamics of a macromolecular machine. *Biochem Soc Trans* **32**, 733-7.
42. Schluenzen, F., Tocilj, A., Zarivach, R., Harms, J., Gluehmann, M., Janell, D., Bashan, A., Bartels, H., Agmon, I., Franceschi, F. & Yonath, A. (2000). Structure

of functionally activated small ribosomal subunit at 3.3 angstrom resolution. *Cell* **102**, 615-623.
43. Korostelev, A., Trakhanov, S., Laurberg, M. & Noller, H. F. (2006). Crystal structure of a 70S ribosome-tRNA complex reveals functional interactions and rearrangements. *Cell* **126**, 1065-77.
44. Ban, N., Nissen, P., Hansen, J., Moore, P. B. & Steitz, T. A. (2000). The complete atomic structure of the large ribosomal subunit at 2.4 A resolution. *Science* **289**, 905-20.
45. Whitford, P. C., Onuchic, J. N. & Sanbonmatsu, K. Y. (2010). Connecting energy landscapes with experimental rates for aminoacyl-tRNA accommodation in the ribosome. *J Am Chem Soc* **132**, 13170-1.
46. Malhotra, A., Tan, R. K. & Harvey, S. C. (1990). Prediction of the three-dimensional structure of Escherichia coli 30S ribosomal subunit: a molecular mechanics approach. *Proc Natl Acad Sci U S A* **87**, 1950-4.
47. Malhotra, A., Tan, R. K. & Harvey, S. C. (1994). Modeling large RNAs and ribonucleoprotein particles using molecular mechanics techniques. *Biophys J* **66**, 1777-95.
48. Villa, E., Sengupta, J., Trabuco, L. G., LeBarron, J., Baxter, W. T., Shaikh, T. R., Grassucci, R. A., Nissen, P., Ehrenberg, M., Schulten, K. & Frank, J. (2009). Ribosome-induced changes in elongation factor Tu conformation control GTP hydrolysis. *Proc Natl Acad Sci U S A* **106**, 1063-8.
49. Tama, F., Valle, M., Frank, J. & Brooks, C. L., 3rd. (2003). Dynamic reorganization of the functionally active ribosome explored by normal mode analysis and cryo-electron microscopy. *Proc Natl Acad Sci U S A* **100**, 9319-23.
50. Wang, Y., Rader, A. J., Bahar, I. & Jernigan, R. L. (2004). Global ribosome motions revealed with elastic network model. *J Struct Biol* **147**, 302-14.
51. Sanbonmatsu, K. Y. & Joseph, S. (2003). Understanding Discrimination by the Ribosome: Stability Testing and Groove Measurement of Codon-Anticodon Pairs. *Journal of Molecular Biology* **328**, 33-47.
52. Sanbonmatsu, K. Y., Joseph, S. & Tung, C. S. (2005). Simulating movement of tRNA into the ribosome during decoding. *Proc Natl Acad Sci U S A* **102**, 15854-9.
53. Sanbonmatsu, K. Y. & Joseph, S. (2003). Understanding discrimination by the ribosome: Stability testing and groove measurement of codon-anticodon pairs. *JOURNAL OF MOLECULAR BIOLOGY* **328**, 33-47.
54. Lim, V. I. & Curran, J. F. (2001). Analysis of codon : anticodon interactions within the ribosome provides new insights into codon reading and the genetic code structure. *RNA-a Publication of the RNA Society* **7**, 942-957.
55. VanLoock, M. S., Agrawal, R. K., Gabashvili, I. S., Qi, L., Frank, J. & Harvey, S. C. (2000). Movement of the decoding region of the 16 S ribosomal RNA accompanies tRNA translocation. *J Mol Biol* **304**, 507-15.
56. VanLoock, M. S., Easterwood, T. R. & Harvey, S. C. (1999). Major groove binding of the tRNA/mRNA complex to the 16 S ribosomal RNA decoding site. *J Mol Biol* **285**, 2069-78.

57. Auffinger, P., LouiseMay, S. & Westhof, E. (1999). Molecular dynamics simulations of solvated yeast tRNA(Asp). *Biophysical Journal* **76**, 50-64.
58. Li, W., Ma, B. & Shapiro, B. (2003). Binding interactions between the core central domain of 16S rRNA and the ribosomal protein S15 determined by molecular dynamics simulations. *NUCLEIC ACIDS RESEARCH* **31**, 629-638.
59. Mears, J. A., Cannone, J. J., Stagg, S. M., Gutell, R. R., Agrawal, R. K. & Harvey, S. C. (2002). Modeling a minimal ribosome based on comparative sequence analysis. *J Mol Biol* **321**, 215-34.
60. Razga, F., Koca, J., Sponer, J. & Leontis, N. B. (2005). Hinge-like motions in RNA kink-turns: the role of the second a-minor motif and nominally unpaired bases. *Biophys J* **88**, 3466-85.
61. Razga, F., Spackova, N., Reblova, K., Koca, J., Leontis, N. B. & Sponer, J. (2004). Ribosomal RNA kink-turn motif--a flexible molecular hinge. *J Biomol Struct Dyn* **22**, 183-94.
62. Ishida, H. & Hayward, S. (2008). Path of nascent polypeptide in exit tunnel revealed by molecular dynamics simulation of ribosome. *Biophys J* **95**, 5962-73.
63. Ge, X. & Roux, B. (2010). Absolute binding free energy calculations of sparsomycin analogs to the bacterial ribosome. *J Phys Chem B* **114**, 9525-39.
64. Vaiana, A. C. & Sanbonmatsu, K. Y. (2009). Stochastic gating and drug-ribosome interactions. *J Mol Biol* **386**, 648-61.
65. Dlugosz, M. & Trylska, J. (2009). Aminoglycoside association pathways with the 30S ribosomal subunit. *J Phys Chem B* **113**, 7322-30.
66. Trylska, J., Konecny, R., Tama, F., Brooks, C. L., 3rd & McCammon, J. A. (2004). Ribosome motions modulate electrostatic properties. *Biopolymers* **74**, 423-31.
67. Chacon, P., Tama, F. & Wriggers, W. (2003). Mega-Dalton biomolecular motion captured from electron microscopy reconstructions. *J Mol Biol* **326**, 485-92.
68. Gao, H., Sengupta, J., Valle, M., Korostelev, A., Eswar, N., Stagg, S. M., Van Roey, P., Agrawal, R. K., Harvey, S. C., Sali, A., Chapman, M. S. & Frank, J. (2003). Study of the structural dynamics of the E coli 70S ribosome using real-space refinement. *Cell* **113**, 789-801.
69. Karplus, M. & McCammon, J. A. (2002). Molecular dynamics simulations of biomolecules. *Nature Structural Biology* **9**, 646-652.
70. Berneche, S., Roux, B. (2001). Energetics of ion conduction through the K+ channel. *Nature* **414**, 73-77.
71. Young, M. A., Gonfloni, S., Superti-Furga, G., Roux, B. & Kuriyan, J. (2001). Dynamic coupling between the SH2 and SH3 domains of c-Src and Hck underlies their inactivation by C-terminal tyrosine phosphorylation. *Cell* **105**, 115-126.
72. Bockmann, R. A. & Grubmuller, H. (2002). Nanoseconds molecular dynamics simulation of primary mechanical energy transfer steps in F1-ATP synthase. *Nature Structural Biology* **9**, 198-202.
73. McCammon, J. A., Gelin, B. R., Karplus, M. (1977). Dynamics of folded proteins. *Nature* **267**, 585-590.

74. Sporlein, S., Carstens, H., Satzger, H., Renner, C., Behrendt, R., Moroder, L., Tavan, P., Zinth, W. & Wachtveitl, J. (2002). Ultrafast spectroscopy reveals subnanosecond peptide conformational dynamics and validates molecular dynamics simulation. *Proc Natl Acad Sci U S A* **99**, 7998-8002.
75. Van Der Spoel, D., Lindahl, E., Hess, B., Groenhof, G., Mark, A. E. & Berendsen, H. J. (2005). GROMACS: fast, flexible, and free. *J Comput Chem* **26**, 1701-18.
76. Trabuco, L. G., Schreiner, E., Eargle, J., Cornish, P., Ha, T., Luthey-Schulten, Z. & Schulten, K. (2010). The Role of L1 Stalk-tRNA Interaction in the Ribosome Elongation Cycle. *J Mol Biol*.
77. Trabuco, L. G., Harrison, C. B., Schreiner, E. & Schulten, K. (2010). Recognition of the regulatory nascent chain TnaC by the ribosome. *Structure* **18**, 627-37.
78. Sanbonmatsu, K. Y. & Joseph, S. (2003). Understanding discrimination by the ribosome: stability testing and groove measurement of codon-anticodon pairs. *J Mol Biol* **328**, 33-47.
79. Garcia, A. E. & Sanbonmatsu, K. Y. (2001). Exploring the energy landscape of a beta hairpin in explicit solvent. *Proteins* **42**, 345-54.
80. Sanbonmatsu, K. Y. (2006). Energy landscape of the ribosomal decoding center. *Biochimie* **88**, 1053-9.
81. Meskauskas, A. & Dinman, J. D. (2007). Ribosomal protein L3: gatekeeper to the A site. *Mol Cell* **25**, 877-88.
82. Baxter-Roshek, J. L., Petrov, A. N. & Dinman, J. D. (2007). Optimization of ribosome structure and function by rRNA base modification. *PLoS One* **2**, e174.
83. Whitford, P. C., Noel, J. K., Gosavi, S., Schug, A., Sanbonmatsu, K. Y. & Onuchic, J. N. (2009). An all-atom structure-based potential for proteins: bridging minimal models with all-atom empirical forcefields. *Proteins* **75**, 430-41.
84. Whitford, P. C., Schug, A., Saunders, J., Hennelly, S. P., Onuchic, J. N. & Sanbonmatsu, K. Y. (2009). Nonlocal helix formation is key to understanding S-adenosylmethionine-1 riboswitch function. *Biophys J* **96**, L7-9.
85. Noel, J. K., Whitford, P. C., Sanbonmatsu, K. Y. & Onuchic, J. N. (2010). SMOG@ctbp: simplified deployment of structure-based models in GROMACS. *Nucleic Acids Res* **38 Suppl**, W657-61.
86. Sanbonmatsu, K. Y. & Garcia, A. E. (2002). Structure of Met-enkephalin in explicit aqueous solution using replica exchange molecular dynamics. *Proteins* **46**, 225-34.
87. Vicens, Q. & Westhof, E. (2003). Crystal structure of geneticin bound to a bacterial 16 S ribosomal RNA A site oligonucleotide. *JOURNAL OF MOLECULAR BIOLOGY* **326**, 1175-1188.